Delayed-choice experiments in quantum interference

T. Hellmuth, H. Walther, A. Zajonc,* and W. Schleich
Sektion Physik, Universität München, D-8046 Garching, Federal Republic of Germany
and Max-Planck-Institut für Quantenoptik, D-8046 Garching bei München, Federal Republic of Germany
(Received 1 October 1986)

Following a suggestion by Wheeler, we have performed delayed-choice experiments in both the spatial and time domains. For the first experiment we use a low-intensity Mach-Zehnder interferometer, and for the second the technique of quantum beats in time-resolved atomic fluorescence. The results obtained show no observable difference between normal and delayed-choice modes of operation, in agreement with the predictions of quantum mechanics.

I. INTRODUCTION

The description of Young's interference experiment in the photon picture has been the subject of extensive discussions in the past. One of the pregnant questions is whether or not the interference pattern formed by integration of many events in which there is only one photon in the apparatus at a time is the same as that obtained with an intense light source.

Experiments to answer this question have been carried out in various arrangements by several authors.[1] With the exception of an experiment by Dontsov and Baz[2] all showed no change of the intensity pattern when the intensity was lowered. In any event the repetition of the Dontsov and Baz experiment later yielded results in accord with the other experiments.[1] Therefore, light seems to exhibit, on the one hand, wave properties and on the other hand it shows the localization pertinent to a particle and demonstrated, for example, by the Compton effect.

We note, however, that these interference experiments have been performed with light from low-pressure discharge lamps. The probability of detecting another photon right after a photon has been measured is given by the second-order correlation function[3] $g^{(2)}(0)$ which in this case is equal to two and thus nonvanishing. The photons have therefore the tendency to arrive in bunches, as known since the pioneering experiments by Hanbury-Brown and Twiss.[4] In a single-photon interference experiment with light from a discharge lamp the probability that a second photon follows immediately after the first one and disturbs the experiment is thus higher than for photons at random. The situation is somewhat improved by the use of laser light since in this case $g^{(2)}(0)=1$. The light ideal for single-photon interference experiments is therefore antibunched light[5] with $g^{(2)}(0)=0$, observed, for example, in resonance fluorescence from atoms of a very diluted atomic beam[6] or from a single ion in an ion trap.[7] So far only one interference experiment using antibunched light has been performed.[8] Here cascading atoms served as a light source for a Mach-Zehnder interferometer. In the same spirit is an experiment currently under way which uses antibunched light provided by an ion in an ion trap so small that only one single ion can get trapped. Photon counting rates of 60 000 counts per second have been achieved.[7] Note also that this experiment does not have the restriction imposed by the statistics of the scatterers in the interaction region with the exciting laser beam important in the experiment of Ref. 8.

According to Bohr,[9] Einstein very early drew attention to a rather striking instance of wave-particle duality, which arises when one attempts to pictorially represent the behavior of a photon in the Young double-slit experiment.[10] Due to its particle character the photon always chooses *one* of the two slits. However, in order to explain the interference structure it is necessary to assume that the photon has traveled *both* paths. Moreover, Einstein proposed to use the linear momentum of the photon at the detector to determine the path of the photon. However, Bohr showed later that the uncertainties in the linear momentum and position of the detector would violate the Heisenberg uncertainty principle. Therefore, it is only possible to observe either the path or the interference of the photon but never both simultaneously.

In this connection an interesting question has been put forward by Wheeler[11] and von Weizsäcker.[12] They ask whether the result of the experiment is changed if the decision for observation of either the path of the photon or interference is made *after* the photon has passed the slits.

Wheeler's delayed-choice *Gedankenexperiment* is summarized in Fig. 1. A pulsed electromagnetic wave is split

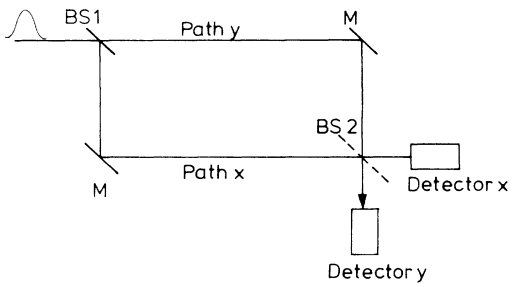

FIG. 1. Schematic diagram of Wheeler's delayed-choice experiment. A single photon pulse enters the interferometer via the beam splitter 1 (BS1). In the absence of the second beam splitter (BS2) the detectors (x and y) ascertain on which "route (path x or path y) the light quantum traveled." Installing the beam splitter 2 this information is irreversibly lost and the two detectors show an interference signature, implying that the light quantum "has traveled both routes." According to Wheeler the insertion of the second beam splitter occurs only *after* the light pulse has entered the interferometer.

into two beams (x and y) by the beam splitter BS1. Two mirrors (M) bring the beams together at the lower right. A detector is placed in each of the two beams (detector for path x and another one for path y). Two experimental situations can be envisioned. In one a second beam splitter (BS2) is introduced at the point of intersection of path x and y. When the path lengths in the two arms of the interferometer are correctly adjusted, no signal appears in one of the counters due to destructive interference, while constructive interference produces a signal at the other detector with the intensity of the beam originally incident on the first beam splitter. This experiment is, as Wheeler puts it, "evidence that the arriving photon came by both routes." In the alternate arrangement the second beam splitter is removed and thus the detectors indicate whether the photon has traveled along path x or y. As in the double-slit experiment it is impossible simultaneously to obtain path information and observe the interference. In the new delayed-choice version of the experiment one decides according to Wheeler "whether to put in the second beam splitter or take it out at the very last minute. Thus one decides whether the photon shall have come by one route, or by both routes after it has already done its travel."

The delayed-choice aspect in interference experiments has attracted considerable attention, and several proposals for experiments have been published.[13–17] In the present article we describe the experimental realization of both a spatial- and a time-domain delayed-choice interference experiment. Preliminary results of these experiments have been published in Ref. 13.

The paper is organized as follows. In Sec. II we decompose the measurement process of the delayed-choice experiment into the different stages[18,19] of state preparation, decomposition, extension of the Hilbert space of the object, and reading. Moreover, we present explicit representations of the noncommuting operators corresponding to path information or interference phenomenon. A delayed-choice experiment in the time domain based on quantum beats is introduced in Sec. III. The experimental setups for the delayed-choice interference as well as the quantum-beat experiments are discussed in Sec. IV. The corresponding experimental results can be found in Sec. V. Finally, Sec. VI is a summary and conclusion.

II. THE DELAYED-CHOICE EXPERIMENT AND THE QUANTUM-MECHANICAL MEASUREMENT PROCESS

In this section we analyze Wheeler's original delayed-choice experiment summarized in Fig. 1 as a quantum-mechanical measurement process in the von Neumann sense.[18,19] This section does not intend to replace a rigorous discussion of the delayed-choice experiment in the language of quantum optics which will be the subject of a future publication.[20] It rather emphasizes the complementarity of the two observables of the photon corresponding to path information or interference phenomenon for which we derive explicit operator representations.

In the following treatment we denote the state vector of a light pulse propagating in the x direction by $|x\rangle$ and similarly for the y direction. The explicit form of $|x\rangle$ or $|y\rangle$ depends on the experimental technique used to produce the pulse.

As discussed later in this paper, the present experiment has been performed using a picosecond laser pulse. Therefore, a laser pulse $|x\rangle$ propagating in the x direction consists[20] of a superposition of $2N+1$ modes being in coherent states[21] $|\alpha_x^{(j)}\rangle$,

$$|x\rangle = |\alpha_x^{(-N)},\alpha_x^{-(N-1)},\ldots,\alpha_x^{(0)},\ldots,\alpha_x^{(N)}\rangle\,|0_y\rangle \tag{1}$$

with a Gaussian frequency distribution

$$\alpha_x^{(j)}=\mathcal{N}e^{-(1/2)\tau^2(\nu^{(j)}-\nu^{(0)})^2}$$

and $j=-N,\ldots,+N$. Here, τ is the pulse duration and the normalization constant $\mathcal{N}$ is

$$\mathcal{N}=\left[2\sqrt{\pi}n\frac{l}{L}\right]^{1/2},$$

where n denotes the number of photons per pulse, L is the length of the cavity of the laser, and $l=c\tau$.

Another experimental technique to produce the single-photon pulse utilizes the resonance fluorescence light from a (two-level) atom in an atomic beam[6] or an ion in an ion trap.[7] In this case the pulse $|x\rangle$ is given[20] by the state vector

$$|x\rangle=\sum_{k_x}\frac{g_{k_x}^*}{\hbar}\frac{1}{(\nu-\omega)+i\gamma}\,|1_{k_x}\rangle\,, \tag{2}$$

where γ denotes the decay rate of the atom, ω is the frequency difference between the two levels, and g describes the coupling to the electric field. The state $|x\rangle$ is thus a superposition of different single-photon states $|1_{k_x}\rangle$ with a Lorentzian frequency distribution.

For the sake of simplicity we confine ourselves in the following discussion to states $|x\rangle$ and $|y\rangle$ such as Eq. (2). In addition, we conclude this section by presenting the results for the interference pattern produced by the picosecond pulse [Eq. (1)].

At the first beam splitter the wave function corresponding to the state $|x\rangle$ is partially transmitted and reflected. The phase of the transmitted part is shifted by ϕ and thus the single-photon state in the interferometer is

$$|\psi\rangle=\frac{1}{\sqrt{2}}(|x\rangle+|y\rangle e^{i\phi})\,. \tag{3}$$

Here we have assumed that the state vectors $|x\rangle$ and $|y\rangle$ are orthogonal and normalized.[22]

The process described so far is the *state preparation*. The succeeding detection process will be described by the expectation values of the object observables.

One such observable is, for instance, the intensity measured by photomultiplier x or y with the second beam splitter being removed. The classical intensities $I_x^{(\mathrm{cl})}$ and $I_y^{(\mathrm{cl})}$ are then

$$I_x^{(\mathrm{cl})}=I_y^{(\mathrm{cl})}=\tfrac{1}{2}\,,$$

where for the sake of simplicity we have set the initial intensity I_0 equal to unity. Using Eq. (3), it is easy to verify

that the operators

$$\hat{I}_x = |x\rangle\langle x| ,$$
$$\hat{I}_y = |y\rangle\langle y| ,$$

indeed yield the above-mentioned classical result. In the basis $\{|x\rangle, |y\rangle\}$ these operators allow a simple matrix representation

$$\hat{I}_x = \begin{bmatrix} 1 & 0 \\ 0 & 0 \end{bmatrix} = \tfrac{1}{2}(\mathbb{1} + \hat{\sigma}_z) ,$$
$$\hat{I}_y = \begin{bmatrix} 0 & 0 \\ 0 & 1 \end{bmatrix} = \tfrac{1}{2}(\mathbb{1} - \hat{\sigma}_z) \tag{4}$$

with the Pauli matrix

$$\hat{\sigma}_z = \begin{bmatrix} 1 & 0 \\ 0 & -1 \end{bmatrix}$$

and the unity matrix $\mathbb{1}$.

Before we turn to the case of the second beam splitter being installed we contrast the path information obtained using the picosecond pulse, Eq. (1), to the one provided by the single-photon state, Eq. (2). In the arrangement of Fig. 1 the route of the photon is determined by either a klick in the detector x indicating that the photon has traveled along path x or in the detector y corresponding to path y. Since a single photon is assumed to be present in the interferometer there should be a perfect anticorrelation in the two detectors. In other words the second-order correlation function $g^{(2)}(0)$ should vanish, i.e., the light should be antibunched as discussed in the introduction. Since the picosecond pulse consists of a superposition of modes being in a coherent state, and therefore $g^{(2)}(0)$ being nonzero, no perfect path information can be obtained. Only antibunched light,[5–7] i.e., the single photon states, Eq. (2), experimentally realized, for example, in the resonance fluorescence light of a single ion stored in a trap[7] provide the means to unambiguously determine the route of the photon (see also Ref. 8).

We now continue the discussion of the measurement process for the case of the second beam splitter being installed. The classical intensities $J_x^{(\mathrm{cl})}$ and $J_y^{(\mathrm{cl})}$ measured at the detectors x and y are then

$$J_x^{(\mathrm{cl})} = \sin^2(\phi/2) ,$$
$$J_y^{(\mathrm{cl})} = \cos^2(\phi/2) . \tag{5}$$

In contrast to the above case it is not so straightforward to find the corresponding operators $\hat{J}_x$ and $\hat{J}_y$. This will be the subject of the remainder of this section.

We start by representing the operators $\hat{J}_x$ and $\hat{J}_y$ by their eigenstates $|s_1\rangle$ and $|s_2\rangle$,

$$\hat{J}_x = \alpha_x |s_1\rangle\langle s_1| + \beta_x |s_2\rangle\langle s_2| ,$$
$$\hat{J}_y = \alpha_y |s_1\rangle\langle s_1| + \beta_y |s_2\rangle\langle s_2| , \tag{6}$$

and similarly the state vector $|\psi\rangle$,

$$|\psi\rangle = c_1 |s_1\rangle + c_2 |s_2\rangle \tag{7}$$

with complex coefficients α_x, α_y, β_x, β_y, c_1, and c_2. The representation of the object state $|\psi\rangle$ as a linear combination of the eigenstates $|s_1\rangle, |s_2\rangle$ is the first step of the quantum-mechanical description of the measuring process and is called *decomposition*.

The next step is the mathematical *extension* of the object Hilbert space H_0 and the apparatus Hilbert space H_A with its pointer basis[23] $|a_1\rangle, |a_2\rangle$ to the product space $H_0 \otimes H_A$.

In the case of the interference observation the apparatus contains the second beam splitter and the detectors x and y. Further discussion will be restricted to the observable $\hat{J}_x$, i.e., only the signal on the detector x is considered. (The treatment of $\hat{J}_y$ is completely analogous.) The detector is characterized by the two macroscopically distinguishable states, the so-called pointer basis,

$$|a_1\rangle = |g\rangle ,$$

where the detector is in the ground state, and

$$|a_2\rangle = |e\rangle ,$$

where the detector is in the excited state. The state of the extended system "object-apparatus" is thus

$$|\Psi\rangle = (c_1 |s_1\rangle + c_2 |s_2\rangle)|g\rangle ,$$

where we have assumed the detector to be in its ground state $|g\rangle$ before the interaction. The interaction of the object with the apparatus transforms the state $|\Psi\rangle$ into

$$|\Psi'\rangle = c_1 |s_1'\rangle |a_1\rangle + c_2 |s_2'\rangle |a_2\rangle .$$

According to von Neumann[18,19] an essential feature of a measuring instrument is that the probability amplitudes c_1 and c_2 of the object state remain unchanged through interaction with the instrument. Moreover, the interaction generates only terms $|s_i'\rangle |a_i\rangle$ $(i=1,2)$ where the states $|s_1'\rangle$, $|s_2'\rangle$ are orthogonal object states, which are not necessarily the same as $|s_1\rangle$, $|s_2\rangle$. Therefore, each state of the pointer basis is uniquely related to an eigenstate of the object.

In the case of the interferometer we get

$$|\Psi'\rangle = c_1 |s_1'\rangle |g\rangle + c_2 |s_2'\rangle |e\rangle . \tag{8}$$

On the other hand, due to the properties of a beam splitter (see Fig. 2), the photon state $|\psi\rangle$ given by Eq. (3) is transformed into the state

$$|\psi'\rangle = \tfrac{1}{2}(1+e^{i\phi})|y\rangle + \tfrac{1}{2}(1-e^{i\phi})|x\rangle . \tag{9}$$

After the interaction with the detector x the state of the whole system object-apparatus is described by

$$|\Psi'\rangle = \tfrac{1}{2}(1+e^{i\phi})|y\rangle|g\rangle + \tfrac{1}{2}(1-e^{i\phi})|0\rangle|e\rangle .$$

Comparison with Eq. (8) yields, for the constants c_1 and c_2,

$$c_1 = \tfrac{1}{2}(1+e^{i\phi}) ,$$
$$c_2 = \tfrac{1}{2}(1-e^{i\phi}) . \tag{10}$$

Inserting Eq. (10) into Eq. (7) determines the state $|\psi\rangle$ of the photons before the second beam splitter. Since this expression must be identical to the one for $|\psi\rangle$ in Eq. (3)

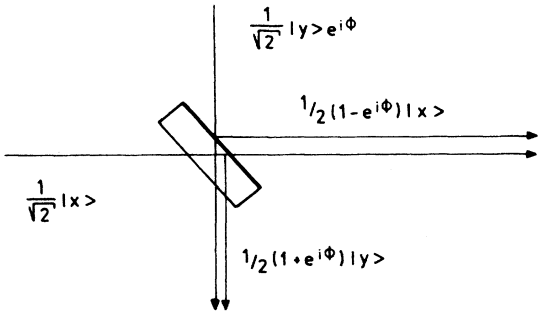

FIG. 2. At beam splitter 2 of the interferometer the two partial waves corresponding to the states $(1/\sqrt{2})|x\rangle$ and $(1/\sqrt{2})|y\rangle e^{i\phi}$ are reflected and transmitted. The phase of the partial wave $(1/\sqrt{2})|y\rangle e^{i\phi}$ is shifted by π since it is reflected at the optically denser medium.

the eigenstates $|s_1\rangle$ and $|s_2\rangle$ can be expressed in terms of the states $|x\rangle$ and $|y\rangle$ via

$$|s_1\rangle=\frac{1}{\sqrt{2}}(|x\rangle+|y\rangle),$$

$$|s_2\rangle=\frac{1}{\sqrt{2}}(|x\rangle-|y\rangle).$$

Substituting this result back into Eq. (6) we arrive at

$$\hat{J}_x=\tfrac{1}{2}\alpha_x(1+|x\rangle\langle y|+|y\rangle\langle x|)+\tfrac{1}{2}\beta_x(1-|x\rangle\langle y|-|y\rangle\langle x|),$$

$$\hat{J}_y=\tfrac{1}{2}\alpha_y(1+|x\rangle\langle y|+|y\rangle\langle x|)+\tfrac{1}{2}\beta_y(1-|x\rangle\langle y|-|y\rangle\langle x|).$$

The constants $\alpha_x,\beta_x,\alpha_y,\beta_y$ can finally be determined by comparing the expectation values to the classical result Eq. (5). It is easy to verify that the operators

$$\hat{J}_x=\tfrac{1}{2}(1-|x\rangle\langle y|-|y\rangle\langle x|),$$

$$\hat{J}_y=\tfrac{1}{2}(1+|x\rangle\langle y|+|y\rangle\langle x|),$$

indeed yield the classical expressions Eq. (5). In matrix representation they take the form

$$\hat{J}_x=\frac{1}{2}\begin{bmatrix}1&-1\\-1&1\end{bmatrix}=\tfrac{1}{2}(\mathbf{1}-\hat{\sigma}_x),$$

$$\hat{J}_y=\frac{1}{2}\begin{bmatrix}1&1\\1&1\end{bmatrix}=\tfrac{1}{2}(\mathbf{1}+\hat{\sigma}_x) \tag{11}$$

with the Pauli matrix

$$\hat{\sigma}_x=\begin{bmatrix}0&1\\1&0\end{bmatrix}.$$

From Eqs. (4) and (11) we observe that the operators $\hat{I}_x,\hat{I}_y$ and $\hat{J}_x,\hat{J}_y$ corresponding to path information or interference phenomenon are noncommuting operators,

$$[\hat{I}_x,\hat{J}_x]=-\frac{i}{2}\hat{\sigma}_y,\quad [\hat{I}_y,\hat{J}_y]=\frac{i}{2}\hat{\sigma}_y$$

with

$$\hat{\sigma}_y=\begin{bmatrix}0&-i\\i&0\end{bmatrix}.$$

The measurement process is completed by the so-called *abstraction* and *reading*. The purpose of the measurement process is to deliver the expectation values of the observables $\hat{J}_x$ and $\hat{J}_y$ as given by Eq. (5).

In the standard version of the interferometer experiment summarized in Fig. 1 the decision which of the observables $\hat{I}_x,\hat{I}_y$ or $\hat{J}_x,\hat{J}_y$ is measured is made *before* the photon enters the interferometer, i.e., *before* the state $|\psi\rangle$, Eq. (3), is prepared. In the delayed-choice mode, however, this decision is made *after* the photon has passed through the interferometer, i.e., *after* the state preparation. In this sense the delayed-choice experiment probes the degree to which state preparation and measurement are independent.

We conclude this section by outlining a discussion on the observation of the interference phenomenon in the language of quantum optics. The intensity $J(\mathbf{r},t)$ measured on a detector located at position $\mathbf{r}$ after the second beam splitter is determined by the correlation function of first order[3]

$$J(\mathbf{r},t)=\langle\psi'|\hat{E}^{(-)}(\mathbf{r},t)\hat{E}^{(+)}(\mathbf{r},t)|\psi'\rangle$$

with the state vector $|\psi'\rangle$ given by Eq. (9) and the positive frequency part of the electric field operator

$$\hat{E}^{(+)}(\mathbf{r},t)=i\sum_{\mathbf{k}}\mathscr{E}_{\mathbf{k}}a_{\mathbf{k}}e^{i(\mathbf{k}\cdot\mathbf{r}-kct)}.$$

Here $k=|\mathbf{k}|$, $\mathscr{E}_k$ is the electric field amplitude per photon,[21] and a_k denotes the annihilation operator. Using the picosecond states $|x\rangle$ and $|y\rangle$ defined in Eq. (1), the intensities J_x and J_y at the two detectors can be calculated[20] and yield

$$J_x=\sin^2(\phi/2)\frac{n}{\sqrt{\pi}}\mathscr{E}_0^2e^{-(1/l^2)(x-ct)},$$

$$J_x=\cos^2(\phi/2)\frac{n}{\sqrt{\pi}}\mathscr{E}_0^2e^{-(1/l^2)(y-ct)},$$

where $\mathscr{E}_0$ denotes the electric field amplitude per photon at frequency $\nu^{(0)}$. Note that this is in agreement with the above simplified treatment.

III. THE DELAYED-CHOICE VERSION OF A QUANTUM-BEAT EXPERIMENT

The delayed-choice aspect of interference in the time domain can be discussed in a way similar to spatial interference. For the experimental observation the quantum-beat method[24] is used.

In the simplest case two energy levels $|a\rangle$ and $|b\rangle$ corresponding to frequencies ω_1 and ω_2 are excited coherently from the ground state $|c\rangle$ with a laser pulse whose pulse duration τ is smaller than the inverse of the characteristic beat frequency $\omega_2-\omega_1$. The state of the system is thus described by a superposition of the two excited states $|a\rangle$ and $|b\rangle$, i.e.,

$$|\psi\rangle=(\alpha|a\rangle+\beta|b\rangle)|0\rangle$$

with complex coefficients α and β. Since initially no photons are present, the electric field is in the vacuum mode $|0\rangle$.

Due to spontaneous emission the two states decay back to the ground state $|c\rangle$ which yields the two paths

$$|c\rangle \rightarrow |a\rangle \rightarrow |c\rangle$$

and

$$|c\rangle \rightarrow |b\rangle \rightarrow |c\rangle \ .$$

Interference between these "routes" results in a modulation of the time-resolved fluorescence intensity I. More precisely, the intensity is given by[24,25]

$$I = \frac{1}{r^2}\Theta(t-r/c)e^{-2\gamma(t-r/c)} \times (\,|\alpha\mathscr{E}_1|^2 + |\beta\mathscr{E}_2|^2 + S\alpha\beta^*\mathscr{E}_1\mathscr{E}_2^* e^{i(\omega_1-\omega_2)(t-r/c)} + \text{c.c.}\,) \ ,$$

where $r = |\mathbf{r}|$ and Θ denotes the Heaviside step function. For the sake of simplicity we have assumed one decay constant γ for the two states. The quantities $\mathscr{E}_1, \mathscr{E}_2$ correspond to electric fields associated with the two transitions and $S=1$.

The analogy to the spatial-interference phenomenon discussed in Sec. II is obvious. In addition, we emphasize the single-photon character of quantum beats; even when many atoms are in the interaction zone the interference is due to a single-photon scattering via two indistinguishable channels. Care must be taken in the measurement process to insure that both channels remain indistinguishable.[25] If one tries to obtain information as to which channel actually participates, using, for example, a filter which transmits only photons of the transition $|c\rangle \rightarrow |b\rangle \rightarrow |c\rangle$, the modulation (interference) disappears and $S=0$.

In this case the observable

$$\hat{\sigma}_+ = |+\rangle\langle +| = \tfrac{1}{2}(\mathbb{1}+\hat{\sigma}_z)$$

is measured where $|+\rangle$ denotes the eigenstate of the circularly polarized photon. Therefore, the observable $\hat{\sigma}_+$ corresponds to $\hat{I}_x$ given by Eq. (4).

If the superposition of both paths is observed the observable

$$\hat{\pi} = \tfrac{1}{2}(|+\rangle + |-\rangle)(\langle +| + \langle -|) = \tfrac{1}{2}(\mathbb{1}+\hat{\sigma}_x)$$

is measured which corresponds to $\hat{J}_y$ defined by Eq. (11). In the delayed-choice version the filter is removed long after each fluorescence photon is emitted, but when the photon has not yet reached the filter.

IV. EXPERIMENTAL SETUP

In this section we discuss the experimental setups for the delayed-choice interference and delayed-choice quantum-beat experiments summarized in Figs. 3 and 4, respectively.

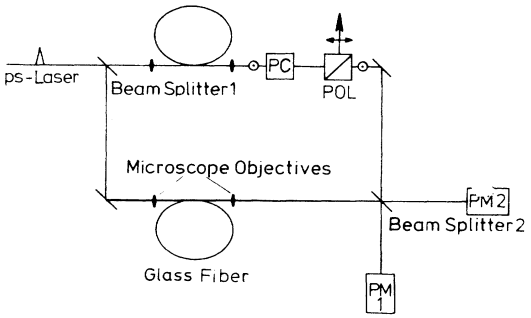

FIG. 3. Setup of the spatial-interference experiment with Pockels cell (PC) and Glan prism polarizer (POL).

A. Delayed-choice interference experiment

Pulses with a pulse duration of 150 ps were produced by an actively mode-locked krypton ion laser (wavelength 647 nm) with a repetition rate of 81 MHz. An acousto-optical switch selected one pulse out of 8000. This reduction in the pulse-repetition rate was necessary since the Pockels cell used to block one of the arms of the interferometer could not be switched more frequently. Furthermore, the reduced pulse frequency guaranteed that the time between two pulses was much longer than the transit time of the light through the interferometer which was about 24 ns. Between the laser and acousto-optic modulator an optical attenuator ($T = 10^{-9}$) was inserted into the laser beam. This ensured that the average number of photons per pulse was less than 0.2.

The incident light passes through the first beam splitter (Fig. 3) and the two beams are then directed and focused into two separate single-mode optical fibers of 5 m in length (core diameter 4 μm). The principal axis of the fibers was aligned such that the polarization of the light leaving the fiber was linear. After recombining the two beams by the second beam splitter the interferences are detected by photomultipliers 1 and 2 (PM1 and PM2) which were cooled to reduce the dark count rate. The intensity recorded in the experiment by each one of the two photomultipliers changed with the path difference in a complementary way having opposite turning points for an optical path difference of $\lambda/2$. Since the path difference of the two arms is strongly influenced by temperature-induced refractive-index variations in the fibers and in the

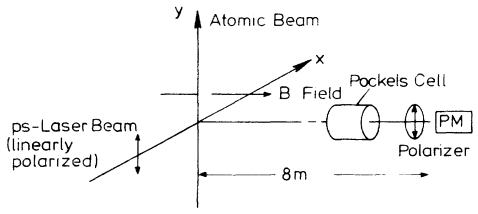

FIG. 4. Schematic arrangement of the quantum-beat experiment.

air the interference pattern changed steadily in time.

To introduce the delayed-choice aspect in the experiment the light path in one arm is interrupted until the photon has passed the first beam splitter. For this purpose a Pockels cell (PC) is installed in the upper arm of the interferometer. To shut off one arm, a voltage is applied to the Pockels cell. As a consequence a phase shift of one-half wave is introduced between two orthogonal polarization components of the incident light, thereby rotating the polarization by 90°. The Pockels cell is followed by a Glan polarizing prism (POL) which deflects the light when the polarization direction is rotated. The rise time of the Pockels cell shutter is 4 ns.

In the experiment the interference pattern of the delayed-choice mode is compared to the "normal" mode. In the normal operation the Pockels cell is open when the light pulse reaches the first beam splitter and is *kept so during the whole transit time through the setup.* In the delayed-choice mode, however, the Pockels cell is normally *closed* and opened 5 ns *after the pulse has passed through the first beam splitter.* Therefore, the light pulse is well inside the optical fiber when the Pockels cell is opened. In order to assume that the Pockels cell is fully open when the light pulse arrives, the length of the fibers had to be sufficiently long. Since the rise time was 4 ns, the length had to be at least 1 m.

An interesting point concerning time ordering in this version of a delayed-choice experiment has been raised and discussed by Mittelstaedt.[26] He stresses the fact that the locations of state reduction, i.e., beam splitter 2, and state preparation, i.e., beam splitter 1, are separated in space. Therefore, expressions such as "switching the Pockels cell before or after the photon has reached the first beam splitter" have to be interpreted using synchronized clocks located at these points. Note, however, that the synchronization procedure only involves the shortest distance between the two beam splitters which in the experiment was smaller than 1 m in contrast to the length of the fiber being 5 m. This guarantees that the normal-choice event occurs in the backward light cone of beam splitter 1.

For data taking the mode of operation was switched between normal and delayed-choice with each successive light pulse. The photons counted by the photomultipliers were stored in different multichannel analyzers accordingly. The switching was controlled by pulses which were derived from the 40.5-MHz driver for the mode locker of the krypton ion laser.

B. Quantum-beat experiment

The quantum-beat experiment was performed using an atomic beam of barium atoms. A magnetic field generated by two Helmholtz coils was applied perpendicular to the direction of the atomic beam (see Fig. 4). Pulses from a synchronously pumped dye laser with a pulse duration of 1.5 ps and repetition frequency of 10 kHz propagate in the x direction. The laser light is polarized in the y direction and its frequency is tuned to the barium resonance line $^1S_0$-$^1P_1$.

Under these conditions a coherent superposition of the two Zeeman sublevels $m=+1$ and $m=-1$ having an energy difference $\Delta E=2\hbar\omega_L$ is populated. Here ω_L is the Larmor frequency (see Fig. 5). The field used was 21 G, corresponding to a splitting which is smaller than the Fourier linewidth of the laser pulses. The fluorescence light is observed time resolved following each laser pulse in the z direction. The collection optics accepted light within a solid angle of 0.1 sr.

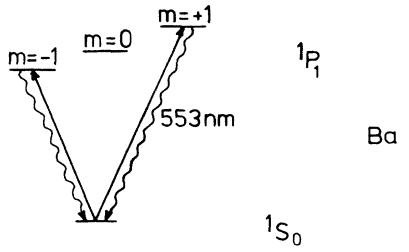

FIG. 5. Excitation scheme of barium used in the quantum-beat experiment.

The time dependence of the signal was measured using a time-to-amplitude converter together with a multichannel analyzer in the pulse-height analyzing mode. This method could be used since there was always less than one photon per laser pulse registered by the detector system. The time-to-amplitude converter was started by the signal of a photocell monitoring the laser pulse, and was stopped by the first signal photon. For the standard quantum-interference experiment a linear polarizer with a polarizing direction parallel to the y direction is placed in front of the photomultiplier. This allows detection of the interference of the two "paths" $|0\rangle\rightarrow|+1\rangle\rightarrow|0\rangle$ and $|0\rangle\rightarrow|-1\rangle\rightarrow|0\rangle$. The delayed-choice version requires that one path remains blocked until the emitted photon arrives at the detection system. For this purpose again a Pockels cell was placed in front of the linear polarizer. If a suitable voltage is applied to the Pockels cell the σ^+ light resulting from the path $|0\rangle\rightarrow|+1\rangle\rightarrow|0\rangle$ is changed into linearly polarized light which is transmitted by the polarizer. The σ^- light is changed into linearly polarized light with a polarization direction perpendicular to the one of the filter and is therefore blocked.

For delayed-choice operation the time of flight of photons between the atomic beam and detection system must be long compared to the rise time of the Pockels cell and the quantum-beat period $\tau=(2\omega_L)^{-1}$. For this reason the light path between atomic beam and detection system was chosen to be 8 m corresponding to a time of flight of 26 ns.

V. EXPERIMENTAL RESULTS

In this section we present the experimental results obtained in the two versions of Wheeler's delayed-choice experiment.

A. Interference experiment

In Fig. 6 we show counts accumulated in a 30-s time interval for photomultiplier 1 [Fig. 6(a)] and photomultiplier 2 [Fig. 6(b)] with alternative light pulses running in

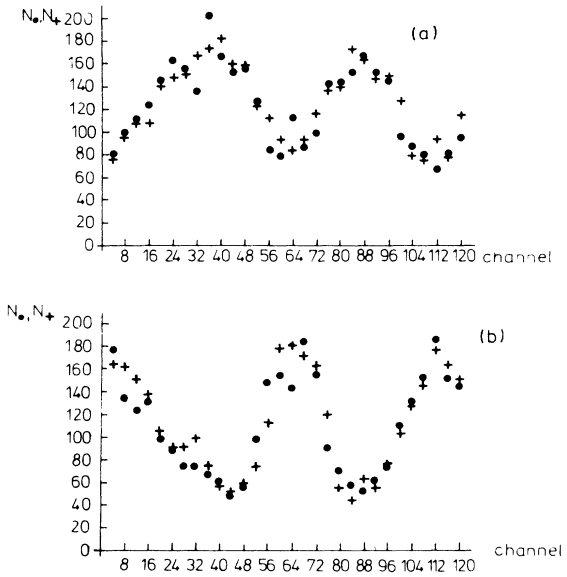

FIG. 6. Comparison of interference patterns for normal and delayed-choice configurations. Dots represent the data taken with the interferometer in its normal configuration, and crosses are data for delayed-choice operation. (a) is for photomultiplier 1, while the phase-inverted signal detected by photomultiplier 2 is shown in (b). The points are four-channel averages of the raw data. The horizontal axis is equivalent to time with 30 s/channel.

the normal (denoted by dots) and delayed-choice modes (indicated by crosses). The resulting counts are stored in a multichannel analyzer operating in the multiscaling mode. The counting was for 30 s/channel. The results shown in Fig. 6 are a four-channel average of the raw data. The time axis is determined by the temperature-induced refractive-index variation within the interferometer. The visibility of the interference patterns in this experiment was reduced from its ideal value of 100%. The origin of this can be related to imperfections of the beam splitters and the detection scheme of the interferences. The light leaving the fibers was collimated by microscope objectives as shown in Fig. 3. Due to the remaining divergence the interference pattern at the output port of the interferometer was a ring system. Only the zeroth-order maximum was detected by the photomultipliers. Due to the finite aperture of the photomultipliers the visibility was reduced.

A more quantitative comparison between the data for delayed and normal modes is achieved by taking the ratio of the corresponding channel counts. These ratios for photomultipliers 1 and 2 are presented in Figs. 7(a) and 7(b), respectively, and yield for the average value

$$N_{\bullet}/N_{+}=1.00\pm0.02$$

and

$$N_{\bullet}/N_{+}=0.99\pm0.02\ .$$

This result is in very good agreement with $N_{\bullet}/N_{+}=1$ predicted by the Copenhagen interpretation[9] of quantum mechanics.

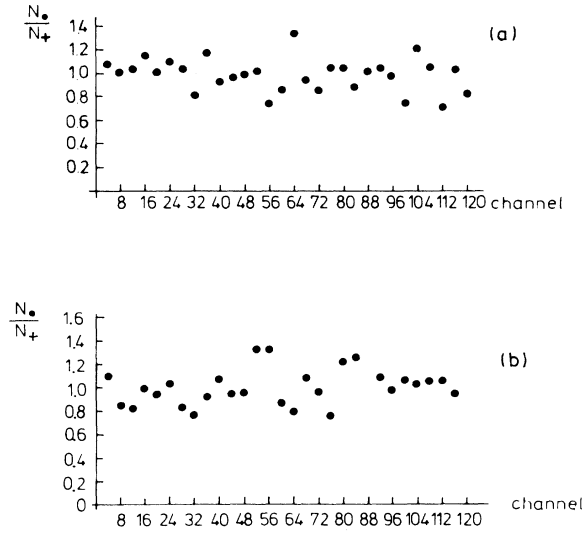

FIG. 7. Ratio $N_{\bullet}/N_{+}$ using the results from Fig. 6. Again the horizontal axis is equivalent to time. The Copenhagen interpretation of quantum mechanics predicts $N_{\bullet}/N_{+}=1$.

B. Quantum-beat experiment

We start by first showing results for the quantum-beat experiment in normal mode. In Fig. 8(a) a quantum-beat signal is obtained without voltage applied to the Pockels cell; in this case a superposition of σ^{+} and σ^{-} light in the fluorescence is observed and the exponential decay is modulated. Applying the quarter-wave voltage to the Pockels cell results in the detection of a single polarized component and thus in the exponential time dependence of the signal as shown in Fig. 8(b). Note that in Figs. 8, 9, and 10 time zero corresponds to the arrival time of the

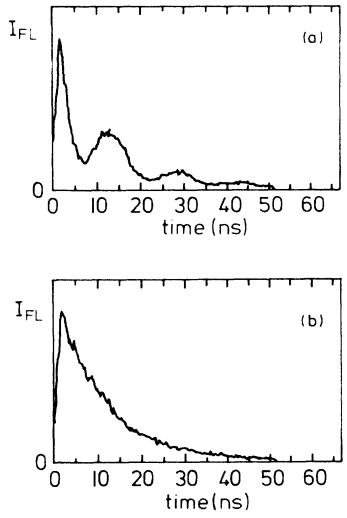

FIG. 8. Time-resolved fluorescence from pulse-excited barium in normal quantum-beat configuration when (a) Pockels cell voltage is zero, (b) a quarter-wave voltage is applied to the Pockels cell.

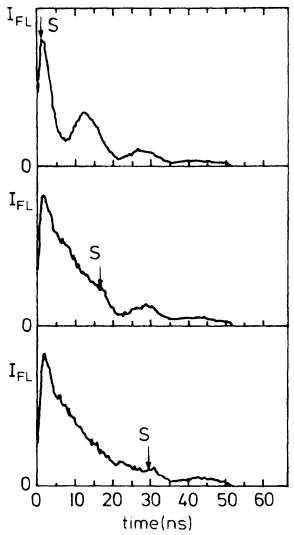

FIG. 9. Time-resolved fluorescence intensity with the Pockels cell switched off at different times (marked by S).

first fluorescence photon at the detector which is 26 ns after the laser pulse. Note also that due to the time resolution of the photomultiplier and the time-to-amplitude converter, the signal reaches its maximum value at about 2 ns.

Results of the delayed-choice version of this experiment are shown in Fig. 9. The arrow marks the time when the voltage was applied to the Pockels cell. Thus for the measurement shown in the upper box the Pockels cell was switched 2 ns after the arrival of the photon at the detector. The middle and lower diagrams show the exponential decay up to 17 and 29 ns, respectively, after which the Pockels cell was switched and the modulation of exponential decay was observed for longer times. In Fig. 10 we compare the usual quantum-beat signal (lower part of Fig. 10) with the one obtained in delayed-choice observation (upper part). Here the voltage at the Pockels cell was switched on at a time of 4 ns (30 ns after the laser pulse). Only that part of the signal which lies between 10 and 30 ns was used in the evaluation. The lower time limit was determined by the rise time of the Pockels cell (4 ns) and the time constant of the detection system (2 ns). The upper limit is determined by the time of flight between atomic beam and detection system.

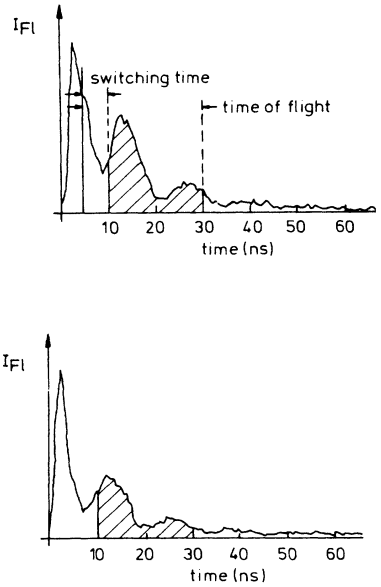

FIG. 10. Comparison of time-resolved fluorescence intensities for the normal (below) and the delayed-choice (above) modes of operation. Only the hatched area is used in evaluation (see text).

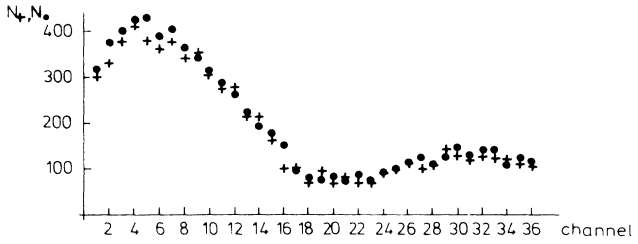

FIG. 11. Quantitative comparison of the hatched area from Fig. 10. Dots represent the delayed-choice and crosses the normal mode of operation. The vertical axis gives the number of counts per channel, and the horizontal corresponds to time with 0.56 ns/channel.

The mode of operation was switched between normal observation and delayed-choice after 10^4 laser pulses. In this way the two signals shown in Fig. 10 were accumulated simultaneously (storing normal and delayed modes in different parts of the multichannel-analyzer memory). The hatched part of the two signals of Fig. 10 are shown in Fig. 11, where the dots correspond to the delayed-choice and the crosses to the normal version. The ratio of the signals in the corresponding channel numbers (time difference 0.56 ns) was calculated. The ratio

$$N_\bullet/N_+ = 1.03 \pm 0.02$$

corresponds again to the one expected from the Copenhagen interpretation. The slight deviation may be due to a slight misalignment of the optical axis of the Pockels cell.

VI. CONCLUSION

The results obtained for the spatial and the time-domain interference experiments described in this paper show no observable difference between normal and delayed-choice modes. They thus confirm the Copenhagen interpretation of quantum mechanics. In this context we note that Alley and collaborators[27] have recently completed a delayed-choice experiment similar to the one discussed in Secs. IV A and V A. Their results were also in agreement with the standard interpretation of quantum mechanics.

We conclude by noting that one way of approaching the logical contradiction inherent in statements concerning photons traveling "one route" or "both routes" is based on quantum logic[26,28,29] which differs substantially from classical logic. Another possibility has been pointed out by Wheeler[11] who noted that it was just "bad use of language" which got us in the dilemma of deciding whether the photon "shall have come by one route, or by both routes" after it has "already done its travel." Reminding us of N. Bohr who introduced the word "phenomenon" into his dialogue with Einstein, Wheeler emphasizes that "No elementary phenomenon is a phenomenon until it is a recorded phenomenon, ... until it has been brought to a close by an irreversible act of amplification such as the blackening of a grain of silver bromide emulsion or the triggering of a photodetector." We therefore have no right to say what "the photon is doing" during its journey in the interferometer. During this time the photon is "a great smoky dragon"[11] which is only sharp at its tail (at the beam splitter 1) and at its mouth where it bites the detector. We conclude by noting that the delayed-choice experiment thus has far-reaching consequences for our picture of the past. As Wheeler has frequently pointed out, the strangeness of the delayed-choice experiment reminds us more explicitly than ever that "the past has no existence except as it is recorded in the present."[10,11]

ACKNOWLEDGMENT

The authors would like to thank C. Alley, P. Mittelstaedt, R. Schlicher, M. O. Scully, G. Süssmann, and J. A. Wheeler for many clarifying discussions on the various subtle aspects of delayed-choice experiments. Financial support of the Deutsche Forschungsgemeinschaft is greatly acknowledged.

---

*On leave from Physics Department, Amherst College, Amherst, MA 01002.

[1]For a review on interference experiments see F. M. Pipkin, Adv. At. Mol. Phys. **14**, 281 (1978); for a discussion of interference between photons from independent sources see H. Paul, Rev. Mod. Phys. **58**, 209 (1986).

[2]Yu. P. Dontsov, and A. I. Baz, Zh. Eksp. Teor. Fiz. **52**, 3 (1967) [Sov. Phys.—JETP **25**, 1 (1967)].

[3]R. J. Glauber, in *Quantum Optics and Electronics,* edited by C. DeWitt, A. Blandin, and C. Cohen-Tannoudji (Gordon and Breach, New York, 1965), p. 63.

[4]R. Hanbury-Brown, and R. Q. Twiss, Nature **177**, 27 (1956); Proc. R. Soc. London Ser. A **242**, 300 (1957); **243**, 291 (1957).

[5]H. J. Carmichael and D. F. Walls, J. Phys. **9B**, L43, 1199 (1976).

[6]H. J. Kimble, M. Dagenais, and L. Mandel, Phys. Rev. Lett. **39**, 691 (1977); Phys. Rev. A **18**, 201 (1978); J. D. Cresser, J. Häger, G. Leuchs, M. Rateike, and H. Walther, in *Dissipative Systems in Quantum Optics,* edited by R. Bonifacio (Springer, Berlin, 1982), p. 21.

[7]F. Diedrich and H. Walther, Phys. Rev. Lett. **58**, 203 (1987).

[8]P. Grangier, G. Roger, and A. Aspect, Europhys. Lett. **1**, 173 (1986).

[9]For an excellent presentation of the Bohr-Einstein dialogue on this subject see in *Quantum Theory and Measurement,* edited by J. A. Wheeler and W. H. Zurek, *Princeton Series in Physics* (Princeton University Press, Princeton, 1983), Chap. 1, and, in particular, the paper by N. Bohr in that book.

[10]For an alternative but interesting picture of the photon in the double-slit experiment as well as in the delayed-choice experiment and the role of the "past" see D. J. Bohm, C. Dewdney, and B. H. Hiley, Nature (London) **315**, 294 (1985).

[11]J. A. Wheeler, in *Mathematical Foundations of Quantum Theory,* edited by A. R. Marlow (Academic, New York, 1978), p. 9; in *Some Strangeness in the Proportion,* edited by H. Woolf (Addison-Wesley, Reading, Mass., 1980), p. 341; in *Problems in the Foundations of Physics,* Proceedings of the International School of Physics "Enrico Fermi," Course LXXII, Varenna, 1977, edited by T. di Francia (North-Holland, Amsterdam, 1979), p. 395; W. A. Miller and J. A. Wheeler, in *Proceedings of the International Symposium on Foundations of Quantum Mechanics,* edited by S. Kamefuchi (Physics Society of Japan, Tokyo, 1983), p. 140.

[12]C. F. von Weizsäcker, Z. Phys. **70**, 114 (1931); **118**, 489 (1941).

[13]T. Hellmuth, A. G. Zajonc, and H. Walther, in *Proceedings of the Symposium on the Foundations of Modern Physics, Joensuu, Finland, June, 1985,* edited by P. Lahti and P. Mittelstaedt (World Scientific, Singapore, 1985); T. Hellmuth, Dissertation, Ludwig-Maximilians-Universität, München, 1985.

[14]W. C. Wickes, C. O. Alley, and O. Jakubowicz, in Ref. 9, p. 457; C. O. Alley, O. Jakubowicz, C. A. Steggerda, and W. C. Wickes, in *Proceedings of the International Symposium on Foundations of Quantum Mechanics,* edited by S. Kamefuchi (Physics Society of Japan, Tokyo, 1983), p. 158.

[15]A. G. Zajonc, Phys. Lett. **96A**, 61 (1983).

[16]M. O. Scully and K. Drühl, Phys. Rev. A **25**, 2208 (1982); M. Hillery and M. O. Scully, in *Quantum Optics, Experimental Gravitation and Measurement Theory,* edited by P. Meystre and M. O. Scully (Plenum, New York, 1983), p. 65.

[17]W. A. Miller, in *Proceedings of the International Symposium on Foundations of Quantum Mechanics,* edited by S. Kamefuchi (Physics Society of Japan, Tokyo, 1983), p. 153.

[18]J. von Neumann, *Mathematische Grundlagen der Quantenmechanik* (Springer, Berlin, 1932).

[19]G. Süssmann, Abh. Bayer. Akad. Wiss. **88** (1958), or in *Observation and Interpretation in the Philosophy of Physics,* edited by S. Körner (Dover, New York, 1962).

[20]W. Schleich, M. O. Scully, and H. Walther (unpublished).

[21]See, for example, M. Sargent, III, M. O. Scully, and W. E. Lamb, Jr., *Laser Physics* (Addison-Wesley, Reading, Mass., 1974).

[22]Note that in general the states $|x\rangle$ and $|y\rangle$ as defined in Eq. (1) are only orthogonal (Ref. 20) for $n \gg 1$, in contrast to the states defined by Eq. (2).

[23]W. H. Zurek, Phys. Rev. D **24**, 1516 (1981).

[24]S. Haroche, in *High-Resolution Laser Spectroscopy,* edited by K. Shimoda (Springer, New York, 1976), p. 253.

[25]W. W. Chow, M. O. Scully, and J. O. Stoner, Phys. Rev. A **11**, 1380 (1975); P. Meystre, M. O. Scully, and H. Walther (unpublished).

[26]P. Mittelstaedt, in *Proceedings of the Second International Symposium on Foundations of Quantum Mechanics,* edited by H. Narumi (Physics Society of Japan, Tokyo, 1987).

[27]C. O. Alley (private communication); O. Jakubowicz, Ph.D thesis, University of Maryland, 1984.

[28]M. Jammer, *The Philosophy of Quantum Mechanics* (Wiley, New York, 1974).

[29]P. Mittelstaedt, *Philosophical Problems of Modern Physics* (Reidel, Dordrecht, Holland, 1976); C. F. von Weizsäcker, Naturwissenschaften **19**, 521 (1955).